

# Dynamic Chest Image Analysis:

## Evaluation of Model-based Pulmonary Perfusion Analysis with Pyramid Images

Jianming Liang<sup>a</sup>, Timo Järvi<sup>a</sup>, Aaro Kiuru<sup>b</sup>, Martti Kormano<sup>b</sup> and Erkki Svedström<sup>b</sup>

<sup>a</sup> Turku Centre for Computer Science, DataCity, Lemminkäisenkatu 14 A, 20520 Turku, Finland

<sup>b</sup> Department of Diagnostic Radiology, Turku University, 20520 Turku, Finland

**Abstract**—Dynamic Chest Image Analysis aims to develop model-based computer analysis and visualization methods for showing focal and general abnormalities of lung ventilation and perfusion based on a sequence of digital chest fluoroscopy frames collected with the Dynamic Pulmonary Imaging technique [18,5,17,6]. We have proposed and evaluated a multiresolutional method with an explicit ventilation model based on pyramid images for ventilation analysis. We have further extended the method for ventilation analysis to pulmonary perfusion. This paper focuses on the clinical evaluation of our method for perfusion analysis. Three clinical cases are included to illustrate the effects of contrast media in perfusion analysis and a dozen of clinical cases without using contrast media are used for evaluation. Our clinical evaluation shows that our method is effective for pulmonary embolism, demonstrating consistent correlations with computed tomography (CT) and nuclear medicine (NM) studies. This performance is the consequence of the idea that the cardiac information recorded in the perfusion image sequence may be utilized to accelerate pulmonary perfusion analysis and improve its sensitivity in detecting pulmonary embolism.

**Keywords**—Chest images, dynamic chest image analysis, pulmonary perfusion, perfusion model, pyramid images.

### I. Introduction

Lungs take air in order to absorb oxygen from air into blood, thus both air and blood flow into the lung are prerequisites to exchange of oxygen from air into blood in the lung. Inadequate function of the lung may be due to failure in *ventilation* or *perfusion* among other factors. In order to detect abnormalities in lung ventilation and perfusion, a number of functional and morphological studies are conventionally used, such as, *ventilation isotope scan* and *perfusion isotope scan*. However, they can only provide a *static*, *coarse* geographic 2D distribution and also have the disadvantage of using radioactive isotopes.

Chest X-ray is the primary imaging method for the diagnosis of pulmonary disorders. Automated analysis of chest X-ray images was one of the first areas to receive attention (e.g., [15,2,3,1,4]). However, previous work is mostly restricted to a single chest image and limited to using spatial information for diagnosis. The information about pulmonary function (ventilation and perfusion) that may be gleaned from a single chest X-ray is rather limited, but it is evident that for effective diagnosis, the function of lungs must be carefully examined.

In recent years, functional imaging has become increasingly prominent as an important new frontier in medical imaging sciences. Turku University Central Hospital has taken the initiative with Dynamic Pulmonary Imaging [18,5,17,6]. A novel image acquisition system has been developed, which can grab a sequence of digital chest fluoroscopy frames at the sampling frequency of 25 Hz in a short period of time (typically, 4.4 seconds). X-rays are attenuated much less in air than in blood and soft tissue; consequently, the average pixel intensity of an area in the lung field varies over time. This variation (called an observation) reflects the air and blood change in the corresponding 2D

projectional area of the lung when the patient breathes naturally, that is, what can be observed is a mixture of the information on both ventilation and perfusion disturbed by noise. This technique opens a new opportunity for pulmonary ventilation and perfusion examination without the use of radioactive isotopes.

Dynamic Chest Image Analysis aims to develop model-based computer analysis and visualization methods for showing focal and general abnormalities of lung ventilation and perfusion based on a sequence of digital chest fluoroscopy frames collected with the Dynamic Pulmonary Imaging technique without using radioactive isotopes. We have proposed and evaluated a multiresolutional method with an explicit ventilation model based on pyramid images for ventilation analysis [10,13]. We have further extended the method for ventilation analysis to pulmonary perfusion [9], where the model parameters are assigned with new medical meanings to form a perfusion model and the pyramid structure is truncated to avoid perfusion artifacts.

In this paper, following the definition of perfusion signals in Section II, we shall review our model-based perfusion analysis with truncated pyramid images in Section III. In order to accelerate pulmonary perfusion analysis and improve its sensitivity in detecting pulmonary embolism, in Section IV, we present a simple yet accurate approach to extract cardiac systolic and diastolic phases from the heart, so that this cardiac information may be utilized to constrain the optimization processes. Three cases are included to illustrate the effects of contrast media in Section V, and a dozen of clinical cases without using contrast media are used for evaluation in Section VI, demonstrating the effectiveness of our technique. We conclude in Section VII.

### II. Perfusion signals

In [10], for a sequence of chest images  $I(x, y, t)$  with  $0 \leq I \leq 255$ ,  $1 \leq x \leq \text{width}$  (192 for ventilation and 384 for perfusion),  $1 \leq y \leq \text{height}$  (144 for ventilation and 288 for perfusion), and  $t$  is a discrete time point in  $[0, \text{examtime}]$  (4.32 seconds for ventilation and 2.04 seconds for perfusion), we have defined a lung functional signal (*i.e.*, an observation) as the average pixel intensity of a region of interest (ROI) over time:

$$O(t) = \frac{\sum_{x,y \in ROI} I(x, y, t)}{|ROI|}. \quad (1)$$

where  $|ROI|$  is the number of the pixels in the region of interest. When the patient breathes naturally, an observation includes both ventilation and perfusion components plus noise. Here, we are only interested in the perfusion component. Therefore, the patient is asked to hold the breath to effectively remove the ventilation component. For convenience, an observation in case of

## Report Documentation Page

<b>Report Date</b> 25 Oct 2001	<b>Report Type</b> N/A	<b>Dates Covered (from... to)</b> -
<b>Title and Subtitle</b> Dynamic Chest Image Analysis: Evaluation of Model-Based Pulmonary Perfusion Analysis With Pyramid Images		<b>Contract Number</b>
		<b>Grant Number</b>
		<b>Program Element Number</b>
<b>Author(s)</b>	<b>Project Number</b>	
	<b>Task Number</b>	
	<b>Work Unit Number</b>	
<b>Performing Organization Name(s) and Address(es)</b> Turku Centre for Computer Science DataCity, Lemminkaiisenkatu 14 A 20520 Turku, Finland		<b>Performing Organization Report Number</b>
<b>Sponsoring/Monitoring Agency Name(s) and Address(es)</b> US Army Research, Development & Standardization Group (UK) PSC 802 Box 15 FPO AE 09499-1500		<b>Sponsor/Monitor's Acronym(s)</b>
		<b>Sponsor/Monitor's Report Number(s)</b>
<b>Distribution/Availability Statement</b> Approved for public release, distribution unlimited		
<b>Supplementary Notes</b> Papers from 23rd Annual International Conference of the IEEE Engineering in Medicine and Biology Society, October 25-28, 2001, held in Istanbul, Turkey. See also ADM001351 for entire conference on cd-rom.		
<b>Abstract</b>		
<b>Subject Terms</b>		
<b>Report Classification</b> unclassified	<b>Classification of this page</b> unclassified	
<b>Classification of Abstract</b> unclassified	<b>Limitation of Abstract</b> UU	
<b>Number of Pages</b> 6		

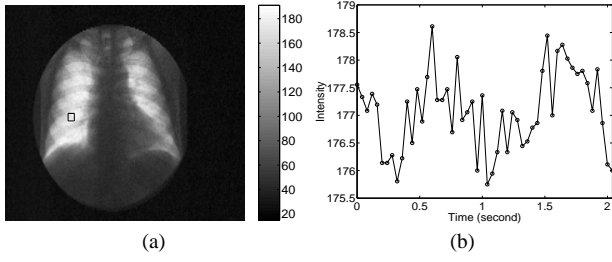


**Fig. 1.** A case with the breath held and an intravenous bolus of X-ray contrast media. (a) An ROI (region of interest) in the right lung field and (b) its corresponding observation – an enhanced lung perfusion signal, which, due to the X-ray physical property, reflects the blood flow in the corresponding lung area with contrast media.

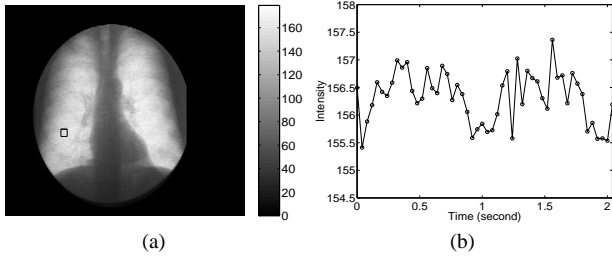


**Fig. 2.** A case with the breath held but no X-ray contrast media. (a) An ROI (region of interest) in the right lung and (b) its corresponding observation – a perfusion signal reflecting the blood flow in the lung area due to the X-ray physical property. It is plotted in the same scale as in Fig. 1 for comparison.

the breath held is called a *perfusion signal*. The perfusion signal strength can be enhanced with an intravenous bolus of X-ray contrast media as shown in Fig. 1. For comparison, Fig. 2 shows a perfusion signal without using contrast media in the same scale.

Pulmonary perfusion analysis is to extract useful perfusion parameters from perfusion signals for showing pulmonary perfusion abnormalities. It is similar to ventilation analysis; consequently, the method we have developed for ventilation analysis would be useful to perfusion analysis. However, perfusion has different properties which should be taken into consideration.

### III. Model-based perfusion analysis with truncated pyramid images

#### A. A perfusion model

For the extraction of perfusion information from a perfusion signal, similarly to ventilation analysis, due to the small number of samples and even poorer signal-to-noise ratio, general signal processing techniques do not work well in the sense of result accuracy. Therefore, the model-based approach becomes more prominent. The perfusion model consists of two sinusoidal functions connected to each other in order to model the non-symmetry of systolic and diastolic phases as depicted in Fig. 3. The model can be expressed as a mathematical function:

$$M(A, D, U, S, L, t) = \begin{cases} A \cos(\pi t' / D) + L & \text{if } 0 \leq t' < D \\ A \cos(\pi(t' - D) / U + \pi) + L & \text{if } D \leq t' < (D + U) \end{cases} \quad (2)$$

where

$$t' = (t - S) \bmod (D + U), \quad (3)$$

and  $t$  indicates *time*. Please note that  $t'$  is always in the interval  $[0, D + U)$ . Mathematically, this perfusion model is the same

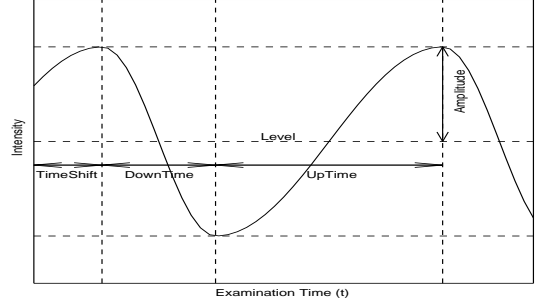


**Fig. 3.** A perfusion model with five free primitive parameters: *amplitude A* (perfusion strength in the lung area), *downtime D* (time for the systolic phase in the lung area), *uptime U* (time for the diastolic phase in the lung area), *timeshift S* (time from the first image to the completion of the first diastolic phase) and *level L* (the mean intensity but with no well-defined medical meaning). This function models the blood change of pulmonary perfusion; it increases during the diastolic phase and decreases during the systolic phase. The systolic phase is generally shorter than the diastolic phase. The free parameters *downtime D* and *uptime U* may be further constrained with the cardiac systolic and diastolic phases extracted from the heart to make the optimization process fast and robust (see Section IV).

as the ventilation model given in [10,13] for ventilation analysis. However, the five characteristic parameters have different medical meanings:

- *Amplitude A*: Perfusion strength.
- *Uptime U*: Time corresponding to the diastolic phase in the lung area.
- *Downtime D*: Time corresponding to the systolic phase in the lung area.
- *Timeshift S*: Time from the first image to the completion of the first diastolic phase.
- *Level L*: Intensity mean – a mathematically necessary parameter without well-defined medical meaning (*i.e.*, its value depending on many factors).

Once a perfusion model is available, the perfusion parameters can be extracted via the nonlinear least squares optimization procedure. The standard algorithm for the nonlinear least squares optimization is the Levenberg-Marquardt method [7,14,16]. This model is sophisticated enough in coverage of both systolic and diastolic phases but remains simple enough for efficient model realization.

#### B. Perfusion properties

When blood flows in the lungs, the phase (*i.e.*, timeshifts) of a pulse signal depends on its location. For observations with different timeshifts, the average/median operator will reduce the amplitude and generate some artifacts. In other words, the amplitude of an observation corresponding to a larger lung area is smaller than that of an observation corresponding to its subpart and it is also more difficult to model the behavior of an observation corresponding to a larger lung area.

For simplicity, let's assume that two adjacent subareas have two pulse signals which are perfect sinusoidal functions with the same amplitude and frequency but different initial phases:

$$p_1 = A \sin(2\pi ft + \theta_1) \quad (4)$$

$$p_2 = A \sin(2\pi ft + \theta_2) \quad (5)$$

where  $A$  is the perfusion amplitude,  $f$  is the pulse frequency, and  $\theta_1$  and  $\theta_2$  are the initial phases of the two pulse signals, respectively. According to the basic properties of trigonometrical

sum, the average pulse for the total area is

$$p = (p_1 + p_2)/2 \quad (6)$$

$$= A \sin[2\pi ft + (\theta_1 + \theta_2)/2] \cos[(\theta_1 - \theta_2)/2] \quad (7)$$

$$= \{A \cos[(\theta_1 - \theta_2)/2]\} \sin\{2\pi ft + [(\theta_1 + \theta_2)/2]\} \quad (8)$$

This naturally implies that as long as  $(\theta_1 - \theta_2)/2 \neq 2\pi \cdot N$ , where  $N = \dots, -1, 0, 1, \dots$ , the amplitude of the pulse signal  $p$  (a new observation) will be smaller than that of the two original pulse signals  $p_1$  and  $p_2$ , and its phase (the average of  $\theta_1$  and  $\theta_2$ ) also differs from those of  $p_1$  and  $p_2$ .

If the pulse signals were perfect sinusoidal functions with the same frequency, we would have another perfect sinusoidal function with the same frequency by the average operator as shown above, although it may have a smaller amplitude and a different initial phase. We may reasonably assume that all pulse signals of a patient during the short examination have the same frequency, but the reality is that the pulse signals are not perfect sinusoidal functions (*i.e.*, the systolic and diastolic phases are not symmetrical). Therefore, the average operator not only reduces the amplitude but also generates some artifacts, since we can not guarantee that a set of the parameters  $(C', A', D', U', S', L')$  satisfy the following equation:

$$\begin{aligned} & M(A, D, U, S_1, L, t) + M(A, D, U, S_2, L, t) \quad (9) \\ &= C' M(A', D', U', S', L', t) \end{aligned}$$

provided that  $D \neq U$  and the difference of  $S_1$  and  $S_2$  is not a cycle length (*i.e.*,  $U + D$ ). In other words, this makes it difficult to model the behavior of an observation corresponding to a larger lung area. We have demonstrated this idea in [8] with artificial signals: The average/median operator reduces the resultant signal's amplitude and also generates some artifacts (*i.e.*, the model cannot be exactly fitted to the resultant signals from the average or median operator).

This means that for perfusion analysis, we need to use higher spatial resolution images in order to avoid the amplitude reduction and the artifacts.

### C. Truncated pyramids

Just like ventilation analysis [10,13], we are interested in not only the overall perfusion function of a lung segment but also its subsegments. This naturally leads to multiresolutional analysis based upon pyramids. The pyramid for each image is obtained by recursively dividing the lung field into 4 (approximately) equal regions till the resulting region is too small to be divided; the intensity value of a pixel (region) in the pyramid is calculated as the average intensity of its corresponding area. This process results in a pyramid of observations. However, because of the perfusion properties discussed in Section III-B, the higher levels of the pyramids should be ignored due to their poorer spatial resolutions. This yields a truncated pyramid where the lowest spatial resolution is still sufficiently high to avoid the amplitude reduction and the artifacts. The truncated pyramid is processed level by level in a top-down fashion to extract the perfusion information from each of its observations.

## IV. Robustly accelerating perfusion analysis with cardiac information

We have formulated the extraction of perfusion parameters as a nonlinear least squares optimization problem. It is well known that the convergence speed and result accuracy depend on the initial guess. Therefore, it is essential to have a good guess when fitting the model to an observation. The truncated pyramid can partially help in this end, since the optimized result of an observation in the truncated pyramid can be taken as an initial guess for its immediate child observations. However, the top level needs to be handled separately. Due to its small signal-to-noise ratio, it is difficult to estimate an initial guess for a perfusion signal. It is also the small signal-to-noise ratio that gives more local minima for the error function in optimization, consequently, it takes more time to converge to a solution. Naturally, it would be desirable if we can reduce the number of free perfusion model parameters, since it not only reduces the optimization time but also improves its stability and result accuracy. In the following, we shall present a simple yet accurate approach to extract cardiac systolic and diastolic phases from the heart, so that this cardiac information may be utilized to constrain the optimization process, making perfusion analysis not only fast but also robust.

### A. Extracting systolic and diastolic phases from the heart

The perfusion examination takes only 2 – 3 seconds, thus, it would be reasonable to assume that the duration of the patient's systolic phase is the same anywhere in the lungs during the examination and so is the duration of the diastolic phase. Consequently, the patient's pulse frequency is the same anywhere in the lungs during the examination. Based on this assumption, we can extract the systolic and diastolic phases from one source: the heart, so that the estimated results of the systolic and diastolic phases can be used as fixed parameters to accelerate the convergence of the optimization processes.

More specifically, first we employ a trick by using an ROI on the heart border as shown in Fig. 4(a) to have an observation (also called a heart signal) (see Fig. 4(b)). The dominant information this observation carries is the change of the heart proportion in the ROI from one frame to another. This signal is generally strong, so the initial guesses for those parameters can be conveniently estimated from the signal itself. The uptime of this signal corresponds to the systolic phase of the heart, while its downtime corresponds to the diastolic phase of the heart. By fitting the perfusion model to this observation, the systolic and diastolic phases are available. Mathematically, from the heart observation  $O_h(t)$ , the fitting can determine a set of parameters  $(A_h^*, D_h^*, U_h^*, S_h^* \text{ and } L_h^*)$  which minimize

$$\sum_{t \in [0, \text{examination time}]} [M(A_h, D_h, U_h, S_h, L_h, t) - O_h(t)]^2. \quad (10)$$

With the United Snakes technique [12,11], we have justified that this simple trick is actually accurate enough in extracting systolic and diastolic phases for pulmonary perfusion analysis [8]. Alternatively, we may use an ROI within the heart area to extract the systolic and diastolic phases. The problem is that such an observation is rather noisy and weak. Moreover, it is com-

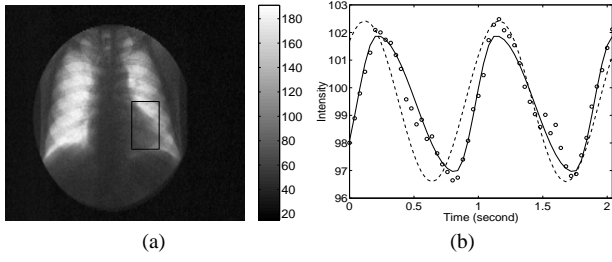


**Fig. 4.** An example for extracting the systolic and diastolic phases from the heart on the case with contrast media. (a) An ROI (region of interest) on the heart border. (b) The corresponding observation and the parameter extraction process. The observation indicated with “o” mainly reflects the change of the heart proportion in the ROI from frame to frame. The initial guess is plotted as dashed curve and the final solution is the solid curve. During the systolic phase, the heart proportion in the ROI becomes smaller and smaller, thus, the average intensity values of the ROI gets bigger and bigger. In other words, the uptime of this signal corresponds to the systolic phase of the heart; while its downtime corresponds to the diastolic phase of the heart — the uptime and downtime extracted from a heart signal have completely different medical meanings from those of an observation in the lung (see Fig. 5). The medical meaning of the extracted amplitude from the heart signal is undefined, since not only does it depend on the heart pumping strength but also the amount of air in the lungs.

plicated in its medical meaning because of the overlapping lung area.

### B. Constraining the fitting process

The estimated systolic and diastolic phases ( $U_h^*$  and  $D_h^*$ ) from the heart signal are then used as fixed parameters in extracting the perfusion parameters from observations in the lung fields (see Fig. 5). However, it should be noted that the uptime and downtime of an observation in the lung fields have completely different meanings from those of the heart signal: the downtime of the signal in the lung areas corresponds to the systolic phase; while its uptime corresponds to the diastolic phase. Mathematically, from the lung signal  $O_l(t)$ , we determine a set of parameters ( $A_l^*$ ,  $D_l^*$ ,  $U_l^*$ ,  $S_l^*$  and  $L_l^*$ ) which minimize

$$\sum_{t \in [0, \text{examtime}]} [M(A_l, D_l, U_l, S_l, L_l, t) - O_l(t)]^2 \quad (11)$$

subject to the constraints:

$$D_l = U_h^*, \quad U_l = D_h^*. \quad (12)$$

Naturally, we always have

$$D_l^* = U_h^*, \quad U_l^* = D_h^*. \quad (13)$$

Therefore, the perfusion analysis gives three parameter images (perfusion amplitude image, timeshift image and level image). As mentioned before, the parameter L (level) has no well-defined medical meaning. Furthermore, we could not see any clear perfusion waves in the lung fields from the timeshift image. We speculate that this is due to the low spatial resolution used in the current research. Therefore, we only use the perfusion amplitude image which appears to be sufficient for diagnosis of pulmonary embolism.

### V. Effects of contrast media

Three clinical cases have been used as experiments for perfusion analysis with contrast media. Due to historical reasons,

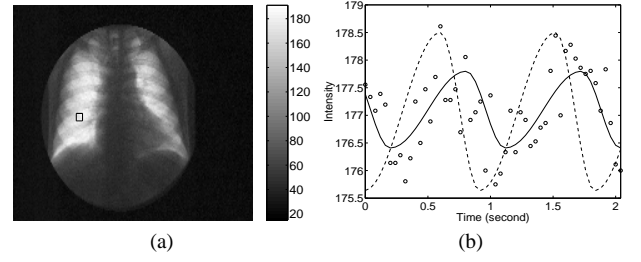


**Fig. 5.** Using the cardiac systolic and diastolic phases to constrain the parameter extraction from an enhanced pulmonary perfusion signal with contrast media. (a) An ROI in the right lung field. (b) The perfusion signal (indicated with “o”) and the parameter extraction process (the dashed curve for the initial guess and the solid curve is the final solution). The downtime of a pulmonary perfusion signal corresponds to its systolic phase (more blood in the lung area); while the uptime corresponds to its diastolic phase (less blood in the lung area).

the image matrix is  $192 \times 144$ , where a pixel corresponds to an area of roughly  $3 \text{ mm} \times 3 \text{ mm}$  of the lung. It is the same spatial resolution as we have used in ventilation analysis [10,13], but the temporal sampling frequency has been doubled (*i.e.*, 25 Hz).

Based on the three perfusion amplitude images in Fig. 6, contrast media concentration in pulmonary vessels appears to have been constant in Case 1, while in Case 2 there is inflow of contrast media into pulmonary arteries causing strong arterial signal and heart motion has caused broader motion artifact than in Case 1. Case 3 represents the inflow period of contrast media through the right subclavian vein and pulmonary arteries with little signal change in pulmonary veins (*e.g.*, early phase after contrast media injection).

This experiment has demonstrated that contrast media can significantly improve the pulmonary perfusion signal strength, but may cause some artifacts disturbing the parameter image interpretation. Furthermore, contrast media are expensive, carry a risk of contrast media reactions, should not be used in patients with pulmonary edema or any renal problem, and also require timing in taking the X-ray series. Therefore, *no* contrast media will be used in clinical evaluation.

### VI. Clinical case studies

In clinical evaluation, we have selected 18 patients, who were referred to this examination mainly to exclude pulmonary embolism. All of them were examined with no contrast media. The image resolution is  $384 \times 288$  pixels and the sampling frequency is 25 Hz. In the following, we shall classify the perfusion abnormal findings into three types and present three representative cases.

#### A. Three types of perfusion abnormalities

We have classified perfusion abnormal findings into the following three types:

- *No perfusion* (NP): The perfusion amplitude is extremely small or zero. This is associated with the complete occlusion of pulmonary arteries by an embolism, and often seen in the upper and middle parts of the lung. When the no-perfusion area becomes larger, likely there will be associated overactive perfusion (OP) in the normal part(s) of the lungs.
- *Reduced perfusion* (RP): The perfusion amplitude becomes smaller than expected and can be seen as darker areas in

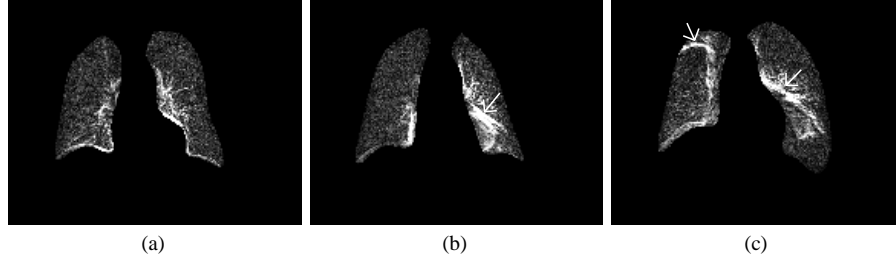


**Fig. 6.** Perfusion amplitude images of three clinical cases with contrast media: (a) contrast media concentration in this case is uniformly distributed. (b) there is an inflow of contrast media into pulmonary arteries causing strong arterial signal (indicated with an arrow). (c) This case represents the inflow period of contrast media through the right subclavian vein and pulmonary arteries indicated with arrows.

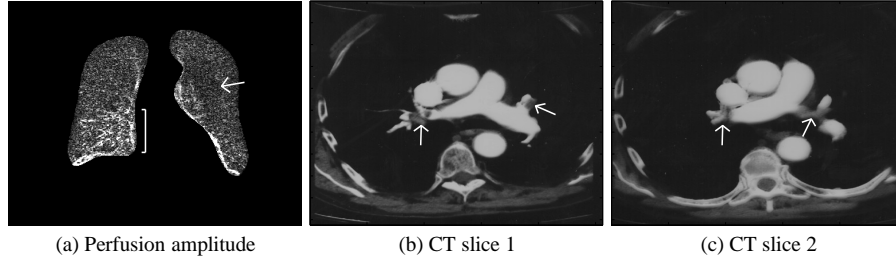


**Fig. 7.** Case 1: (a) Overactive perfusion (OP) is seen in the right lower lung field (indicated with a bracket), while slightly reduced perfusion (RP) is shown in the rest of the right lung. Reduced perfusion (RP) is revealed in the central part of the left lung (indicated with an arrow). The CT images (b, c) of the same patient show embolic masses partially filling the right pulmonary artery and also material in the left lower lobe artery (indicated with arrows). Our findings also show a good correlation with the patient's clinical report of the NM study performed in another hospital (the NM image is not available).

the perfusion amplitude image. This is the typical phenomenon of pulmonary embolism with partial occlusion.

- *Overactive perfusion (OP)*: The perfusion amplitude is bigger than expected and the area should be considered as normal. This is the phenomenon caused by the excessive blood flow redirected into the normal area due to no-perfusion and reduced perfusion in other parts of the lungs.

The lung field may be visually divided into three regions (upper, middle and lower). The statistics of perfusion abnormalities found in the 18 patients are summarized in Table 1.

Right/Left	NP	RP	OP
Upper	2/3	5/5	1/1
Middle	2/1	3/3	0/9
Lower	1/2	7/2	1/3

**Table 1.** Statistics of perfusion abnormalities.

### B. Three representative clinical cases

Illustrated here are three representative cases, who were also examined with computed tomography (CT) and pulmonary perfusion nuclear medicine (NM). Both CT and NM are the “golden standard” method in detection of pulmonary perfusion disturbances (e.g., pulmonary embolism). NM shows the distribution of pulmonary perfusion, while CT reveals the thrombotic masses causing pulmonary embolism.

- Case 1 (see Fig. 7): Pulmonary embolism of the right middle lobe and the right upper lobe is associated with reduced perfusion (RP) in the middle and upper fields of the right lung. In addition, there is reduced perfusion (RP) in the left upper lobe and perihilar region of the left lower lobe. The reason for a very high amplitude (overactive perfusion, OP) in the right lower lung field is due to the high concentration of the blood in this area. These findings show a good correlation with both CT and NM studies.
- Case 2 (see Fig. 8): Pulmonary embolism in the right lung

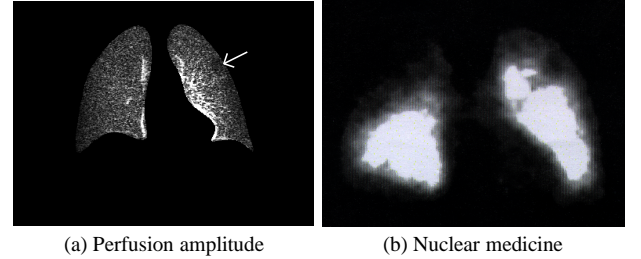


**Fig. 8.** Case 2: (a) Overall reduced perfusion (RP) of the right lung. Overactive perfusion (OP) is seen centrally in the left lung, while reduced perfusion (RP) is shown in the left apex and a small area (indicated with an arrow) in the upper left lung field. Pulmonary embolism in the right lung and in the superior segment of the left lower lobe shown by CT and NM (b) studies. Generally, the NM image shows the perfusion activity in the anterior parts of the lungs, while our perfusion amplitude image reveals perfusion through the lungs. Therefore, the reduced perfusion of the lower part of the right lung shown by our method (a) may be explained by the thrombotic mass in the hilar region of the right lung as reported by CT.

and in the superior segment of the left lower lobe shown by CT and NM studies is correlated to reduced perfusion (RP) of the right lung and reduced perfusion (RP) of the left apex and a small area in the upper left lung field. Overactive perfusion (OP) is seen centrally in the left lung.

- Case 3 (see Fig. 9): Generally reduced perfusion (RP) of the right lung and no perfusion (NP) of the lateral recess in the left lung. These findings are consistent with CT and NM studies. Overactive perfusion (OP) seen centrally in the left lung is due to the redirection of blood flow.

The clinical case studies show that our model-based method for pulmonary perfusion analysis is effective for pulmonary embolism even without using contrast media, demonstrating consistent correlations with CT and NM studies. This gives our present technique some advantages. It takes only about 2 seconds and involves *no* radioactive isotopes, *no* contrast media and only *low* radiation dose [6,5,17]. The NM study takes much



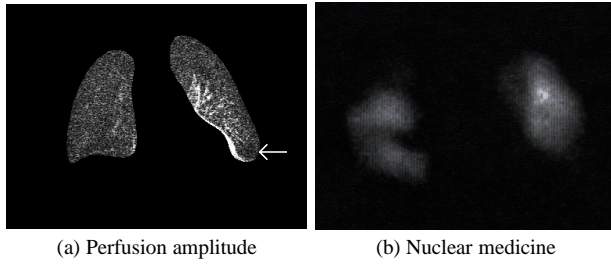


**Fig. 9.** Case 3: (a) Generally reduced perfusion (RP) of the right lung. No perfusion (NP) of the lateral recess in the left lung (indicated with an arrow). Overactive perfusion (OP) seen centrally in the left lung. These findings are consistent with CT and NM (b) studies.

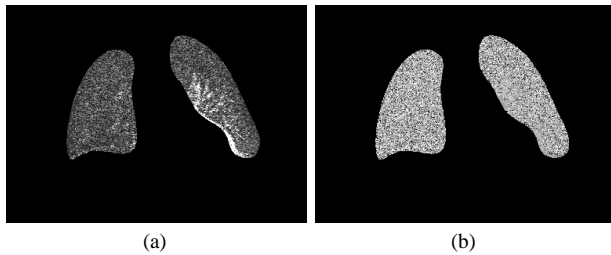


**Fig. 10.** Case 3: (a) Perfusion amplitude image and (b) perfusion frequency image obtained from an analysis without using cardiac information. Compared with the amplitude image in Fig. 9(a), this amplitude image (a) is rather noisy in the no-perfusion and reduced perfusion areas. The no-perfusion area of the lateral recess in the left lung is not so visible as that in Fig. 9(a). The no-perfusion and reduced perfusion areas in the perfusion frequency image (b) are also noisy.

longer (over 20 minutes) and it is not readily available in any hospital. The CT study uses high amount of contrast media and has side effects. Furthermore, CT is expensive and cannot be used for all patients (*e.g.*, anxiety and contrast media reactions).

This performance of our computer analysis method is the consequence of the idea of reducing the number of free perfusion model parameters (see Section IV), which makes the optimization process not only fast but also robust in computation. For comparison, we have performed a test on Case 3 without constraining uptime and downtime with the cardiac information. It takes about 10 times longer and the results are rather sensitive to noise, specially in the no-perfusion and reduced perfusion areas as shown in Fig. 10. Perfusion analysis is to show pulmonary perfusion abnormalities (*i.e.*, no-perfusion and reduced perfusion). In a reduced perfusion area, the signal component with the pulse frequency is weak, while, in a no-perfusion area, its observation has no such a component. When the uptime and downtime are constrained, the extraction process will only search for the component with the pulse frequency in the observation, consequently, it will be able to quickly and robustly give a small value or zero to the amplitude parameter in the reduced perfusion area or no-perfusion area without being disturbed by noise.

## VII. Conclusion

We have extended our method for ventilation analysis to pulmonary perfusion analysis. According to perfusion properties, we have assigned new medical meanings to our model parameters in order to form a perfusion model and truncated the pyramid structure so as to avoid perfusion artifacts.

Three clinical cases have been used to illustrate the effects of contrast media. To enable comparison with computed tomography (CT) and nuclear medicine (NM) studies, perfusion abnor-

mal findings are classified into three types. The clinical evaluation has shown that our computer analysis method is effective for pulmonary embolism even without using contrast media, demonstrating consistent correlations with CT and NM studies. This performance is the consequence of the idea that the cardiac information recorded in the perfusion image sequence may be utilized to accelerate pulmonary perfusion analysis and improve its sensitivity in detecting pulmonary embolism. In doing so, a simple yet accurate approach has been introduced to extract cardiac systolic and diastolic phases from the heart for constraining the optimization processes. This idea has not only made perfusion analysis fast but also robust; consequently, perfusion analysis becomes feasible without using contrast media.

## References

- [1] D. H. Ballard. *Hierarchical Recognition of Tumors in Chest Radiographs with Computer*. Basel, 1976.
- [2] H. C. Becker, *et al.* Digital computer determination of a medical diagnostic index directly from chest X-ray images. *IEEE Trans. Biomed. Eng.*, 11:67–72, 1964.
- [3] Y. P. Chien and K.-S. Fu. Recognition of X-ray picture patterns. *IEEE Transactions on Systems, Man, and Cybernetics*, 4(2):145–156, 1974.
- [4] M. L. Giger, *et al.* An “intelligent” workstation for computer-aided diagnosis. *RadioGraphics*, 13:647–656, 1993.
- [5] A. Kiuru, E. Svedström, and I. Kuuluvainen. Dynamic imaging of pulmonary ventilation: Description of a novel digital fluoroscopic system. *Acta Radiologica*, 32:114–119, 1991.
- [6] A. Kiuru, E. Svedström, J. Mäki, and K. Kärpjoki. Dynamic pulmonary ventilation imaging: Clinical usage with Windows interface. In *CAR’96: Computer Assisted Radiology*, pages 179–184, 1996.
- [7] K. Levenberg. A method for the solution of certain problems in least squares. *Quart. Appl. Math.*, 2:164–168, 1944.
- [8] J. Liang. *Dynamic Chest Image Analysis*. Turku Centre for Computer Science, Turku, Finland, December 2000. [TUCS Dissertation No. 31].
- [9] J. Liang, A. Haapanen, T. Järvi, A. Kiuru, M. Kormano, E. Svedström, and R. Virkki. Dynamic chest image analysis: Model-based pulmonary perfusion analysis with pyramid images. In E. A. Hoffman, editor, *Medical Imaging 1998: Physiology and Function from Multidimensional Images*, pages 63–72, San Diego, CA, 1998.
- [10] J. Liang, T. Järvi, A. Kiuru, M. Kormano, E. Svedström, and R. Virkki. Dynamic chest image analysis: Model-based ventilation study with pyramid images. In E. A. Hoffman, editor, *Medical Imaging 1997: Physiology and Function from Multidimensional Images*, pages 81–92, Newport Beach, CA, 1997.
- [11] J. Liang, T. McInerney, and D. Terzopoulos. Interactive medical image segmentation with united snakes. In *Proc. Second International Conf. on Medical Image Computing and Computer-Assisted Intervention (MICCAI 99)*, pages 116–127, Cambridge, England, September 1999. Springer.
- [12] J. Liang, T. McInerney, and D. Terzopoulos. United snakes. In *Proc. Seventh International Conf. on Computer Vision (ICCV’99)*, pages 933–940, Kerkira (Corfu), Greece, September 1999. IEEE Computer Society Press.
- [13] J. Liang, R. Virkki, T. Järvi, A. Kiuru, M. Kormano, and E. Svedström. Dynamic chest image analysis: Evaluation of model-based ventilation study with pyramid images. In R. Zurawski and Z.-Q. Liu, editors, *IEEE First International Conference on Intelligent Processing Systems*, pages 989–993, Beijing, China, 1997.
- [14] D. W. Marquardt. An algorithm for least-squares estimation of nonlinear parameters. *SIAM J. Appl. Math.*, 11:431–441, 1963.
- [15] P. H. Myers, C. M. Nice, H. C. Becker, W. J. Nettleton, J. W. Sweeney, and G. R. Mechstroth. Automated computer analysis of radiographic images. *Radiology*, 83:1029–1033, 1964.
- [16] L. E. Scales. *Introduction to Non-Linear Optimization*. Macmillan Publishers Ltd, 1985.
- [17] E. Svedström. *Dynamic Pulmonary Imaging: Development and evaluation of a new technique with a special reference to pediatric ventilation studies*. Turku University, March 1992. [Academic Dissertation Med.-Odont. 89].
- [18] E. Svedström, A. Kiuru, and H. J. Puhakka. Dynamic imaging of pulmonary ventilation using digital subtraction radiography. *Acta Radiologica (Diagn)*, 31:53–58, 1990.